Magnetoresistance of a domain wall at a submicron junction

Y. B. Xu, C. A. F. Vaz, A. Hirohata, H. T. Leung, C. C. Yao, and J. A. C. Bland
Cavendish Laboratory, University of Cambridge, Cambridge CB3 0HE, United Kingdom

E. Cambril, F. Rousseaux, and H. Launois
L2M/CNRS, 19 Avenue Henri Ravera, 92220 Bagneux, France

(Received 8 February 2000)

A local magnetoresistance (MR) effect associated with the switching of a coherent spin block confined in a cross-shaped junction of mesoscopic ferromagnetic NiFe wires was probed with the voltage pads attached close (<1.5 μm) to the junction. A positive intrinsic MR effect, i.e., an increase in resistance, associated with local spin noncollinearity, or a 45° domain wall, in a 0.5 μm cross was demonstrated while the anisotropic MR and the Lorentz MR were unambiguously excluded.

The spin configurations of magnetic domain walls (DW) in ferromagnets have the same feature of noncollinearity found in antiferromagnetically coupled magnetic multilayers or magnetic granular systems, both of which display giant magnetoresistance (GMR).[1] Accordingly, spin-dependent transport effects associated with the presence of the DW are expected. This idea was explored by Gregg *et al.*[2] and a positive magnetoresistance (MR) effect due to DW scattering was observed in continuous Co films with regular stripe domains. Hong and Giordano[3] observed discontinuous changes of the resistance upon sweeping the field in Ni wires. This was attributed to the nucleation and movement of DW, which transverse the wire during magnetization reversal. Rüdiger *et al.*[4] has investigated the effect of the domain wall on the MR in micron size Fe wires with a controlled stripe domain structure. A negative MR effect was identified at the temperature where the anisotropic MR (AMR) and Lorentz MR compensate each other. The negative MR effect of DW was also observed by Ohtani *et al.*[5] in wires with a ''neck.'' Several theoretical models[6–9] based on new physical mechanisms have been proposed to explain the experimental observations. Levy and Zhang[6] calculated the spin flip, as well as nonflip scattering present in DW with the same Hamiltonian used to explain the GMR effect. The positive MR observed in continuous Co films was attributed to an admixture of spin states in the presence of the DW. van Hoof[8] made *ab initio* calculations of the specular electron transmission through DW and proposed that the MR effect of the DW is due to the change in the electronic band structure of the ferromagnets brought about by spin rotation. Tatara and Fukuyama[7] on the other hand found that the DW contributes to the decoherence of electrons and the nucleation of a wall leads to a decrease of resistance (negative MR) in the weakly localized regime which occurs at less than about 20 K. More recently, Lyanda-Geller *et al.*[9] discussed the importance of the electron-electron interaction quantum corrections and universal conductance fluctuations along with weak localization for the electron transport through regions of spatially varying magnetization, such as domain walls. We can see from the above arguments that there are striking disagreements between the different experimental reports as well as between the various proposed theoretical models concerning the sign, the temperature range, and the mechanism causing the MR effect. These conflicting theoretical and experimental studies now call for further observations of the DW MR under conditions in which domain structure can be well defined and both the Lorentz MR and AMR effects excluded.

Nanofabrication of mesoscopic magnets provides a key opportunity to address this spin-dependent electron-transport effect associated with the local spin noncollinearity, as the domain structure can be controlled by varying the shape and lateral dimensions. In this paper, we have designed and fabricated a simple cross shape wire structure using advanced *e*-beam lithography. The electric pads were fabricated to be as close as possible to the junction of the crosses to probe the local MR response of regions with controlled spatially varying magnetization. The aim was to confine domain walls in a junction of submicron size and to clarify unambiguously the intrinsic MR effect due to spin noncollinearity.

Continuous films of Au(30 Å)/$Ni_{80}Fe_{20}$(300 Å)/GaAs(100) used for the patterning were deposited in an UHV system. The substrate was held at 30 °C during growth and was then annealed at 120 °C for 30 min to remove the uniaxial anisotropy. The Au/NiFe layer was patterned by electron-beam lithography (JEOL JBX5D2U) operated at 50 KeV and etched by ion beam etching (IBE) with an intermediate metallic mask of Al made by a liftoff process. Two sets of mesostructures were fabricated. One is a set of straight wires with width $w=0.2$, 0.5, 1, 2, 5, and 10 μm and length fixed at 200 μm, the other one is a set of crosses with two wires of the same width joined perpendicularly together. Figure 1(a) is a scanning electron micrograph (SEM) of a 0.5 μm cross around the junction area. Electrical contacts for the transport measurements were made of Cr(20 nm)/Au(300 nm) patterned by *e*-beam lithography with careful positioning. Some of the electrical contacts were extended with large Al pads for better bonding. As shown in Fig. 1(b), there are eight pads connected to each cross sample for MR, as well as Hall-effect measurements. A dc current of 50 μA was passed through both ends of the wires. The voltage probes [as shown clearly in Fig. 1(a)] were placed very close ($\sim$1.5 μm) to the junction for local MR measurements. The magnetic field was applied in the plane of the samples. The field was applied parallel and perpendicular to the current for the

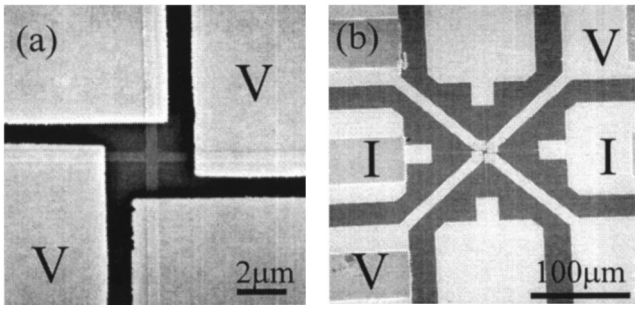

FIG. 1. (a) SEM micrograph around the junction area of a 0.5 μm width cross, and (b) large-scale micrograph showing the electrical contact geometry.

longitudinal MR (LMR) and transverse MR (TMR) measurements, respectively. All the measurements were carried out at room temperature. The domain imaging was carried out with a Nanoscope III using a low stray field tip for magnetic force microscopy (MFM).

The domain structures of both the wires and crosses have been imaged in zero external field. The images are reproducible and represent the domain structures of the stable configurations at minimum magnetic energies. MFM images of NiFe straight wires show that the domain width in these wires is about 1 μm and the submicron wires are in a single domain state. The images of the cross samples were collected rather close to the junction region, which is also chosen to avoid the large voltage pads. The domain structures of the few micron-size structures were found to split into multidomain states with several domain walls across the junction area. With decreasing wire width, the number of domains and domain walls formed around the junction decreases. Figures 2(a) and 2(b) are the MFM images of 0.5 μm and 1 μm crosses, respectively. A single domain state can be identified from the absence of contrast in the wire region. The spins in the wire region are aligned along the wire direction due to the strong shape anisotropy. However, the images show significant contrast across the junction area with diagonal patterns visible. This result indicates the confinement of domain walls around the junction of the crosses.

Micromagnetic calculations have been used to simulate the images observed and to determine the detailed domain configuration around the junction. The simulated region is 10 μm$\times$10 μm, i.e., the full length of the arms from one side to the other is 10 μm. The samples were divided into cubic cells of $(30\ \text{nm})^3$ with exchange constant $A=1.0\times10^{-6}$ erg/cm, and magnetization $M_s=923$ emu/cm^3. We have chosen the starting condition such that the junction region of about 3×3 μm^2 is completely random while the initial magnetization in the middle of the arms are preferentially aligned along the wire direction. This is justifiable as in the real samples with the arms of 100 μm in length the strong shape anisotropy will keep the spin aligned along the wire direction. Figures 2(c) and 2(d) show the simulated MFM images (corresponding to $\nabla\cdot\mathbf{M}$)for the 0.5 μm and 1 μm crosses around the junction. The detailed magnetization configuration is shown in Fig. 3(a), along with the simulated current distribution in Fig. 3(b). A ''parallel'' state in which the spins of the arms on opposite sides of the junction are oriented parallel was found to be the most stable state, while the ''antiparallel'' state (or ''head to head'' as described in our

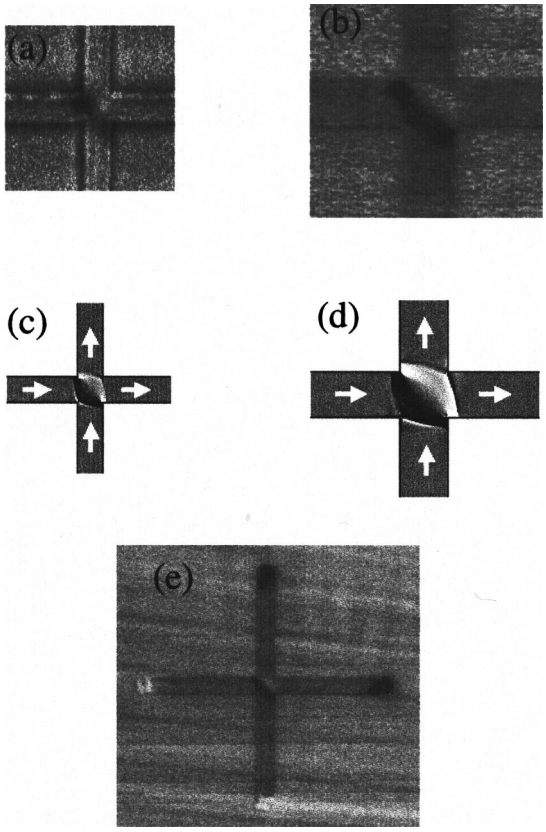

FIG. 2. MFM images around the junction area of (a) 0.5 μm, and (b) 1 μm crosses, and simulated MFM patterns corresponding to values of $\nabla\cdot\mathbf{M}$ for (c) 0.5 μm, and (d) 1 μm crosses. A large scale MFM image from a 1 μm cross (the arm length is 10 μm) is included in (e), which shows the charges at the ends.

preliminary work[10]) is a metastable state. Both the simulated images show a rather similar pattern of a change in contrast across a diagonal line, which agrees well with the key feature of the MFM images observed. As a further check, in Fig. 2(e) we show a large scale MFM image of a 1 μm width and 10 μm length cross structure. The charges observed at the wire ends confirm the simulations. Figure 3(a) shows that the spin rotates by 45° from the arms to the junction, and all the spins within the junction are aligned approximately along the diagonal direction. The junction can thus be described as a giant coherent spin block (CSB). A 45° domain wall is formed between each arm and the junction. The confinement of a CSB at the junction is due to the reduction of the junction size, which resembles the formation of a single domain particle.

The conventional sources of MR in these wire structures, namely AMR and Lorentz MR, have been assessed by measuring the MR effect of the reference samples of straight wires. The LMR of the multidomain micron size wires is determined by the AMR effect, which is similar to that observed in multidomain NiFe wires.[11] The LMR of the submicron size wires, however, is very small and no MR effect contributed from the magnetization reversal was seen as shown by the MR curve of a 0.5 μm wire in Fig. 4(a). For a single domain wire, the magnetization **M** is either parallel or antiparallel to the current direction **I** and no AMR effect is expected. As the AMR effect was suppressed in this single domain wire, the intrinsic Lorentz MR was seen clearly at

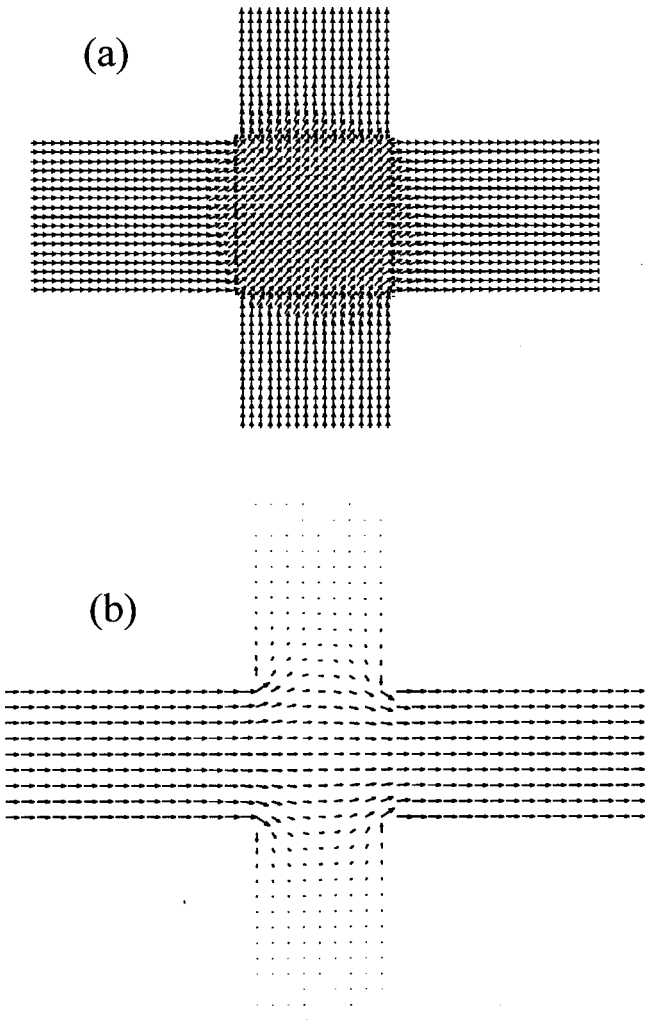

FIG. 3. (a) Detailed domain configuration **M** around the junction of the 0.5 μm cross from the micromagnetic calculations (the corresponding $\nabla \cdot \mathbf{M}$ is shown in Fig. 2(c), and (b) current distribution calculated using a finite element method. Similar results were obtained for the 1 μm cross.

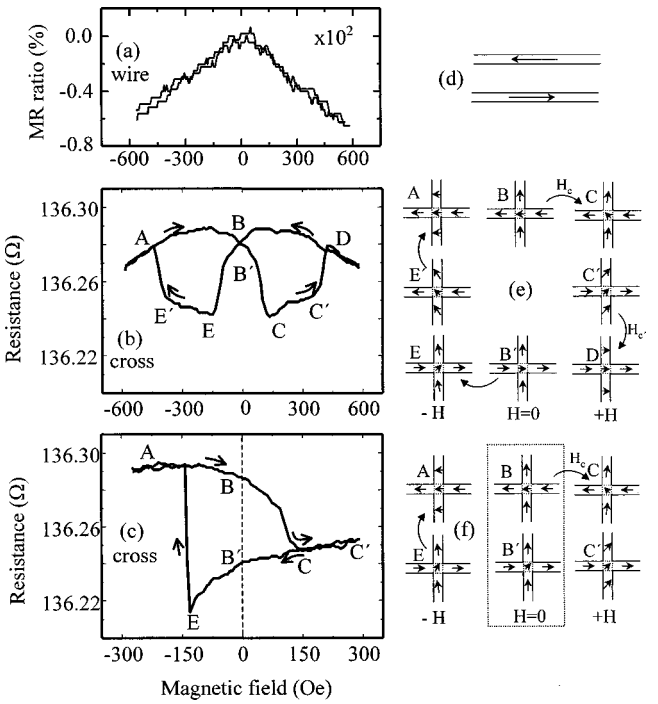

FIG. 4. The longitudinal MR curves of (a) the 0.5 μm straight wire, (b) the 0.5 μm cross, and (c) the 0.5 μm cross with the maximum applied field reduced to about 300 Oe starting from the saturation state *A*. (d)–(f) schematics of the corresponding domain configurations.

low field with our high-resolution MR measurements. The resistance of the 0.5 μm wire varies linearly with magnetic field with a very small slope of about 1×10^{-5} per 100 Oe. The TMR of both the wires and crosses has also been measured. The TMR values [about $1.4\pm0.1\%$ (Ref. 10)] were found to be approximately independent of the widths and the shape of the samples as expected from the AMR effect.

Figures 4(b) and 4(c) show the LMR of the 0.5 μm cross sample, which suggests the importance of the junction to magnetotransport properties. The magnetic field was swept between -600 to 600 Oe in Fig. 4(b). Two striking features can be seen from this figure: (i) the resistances at points A, B, B′, and D are approximately the same, and (ii) the curve shows two jumps, namely B-C, and C′-D in the reversal magnetization process. When the field is reduced to zero from the saturation, the spins of the vertical arms rotate from the horizontal direction at point A to the vertical direction at point B, i.e., along the wire direction, as shown by a schematic diagram in Fig. 4(e). The similar resistance of points A and B shows that the switching of the vertical arms contributes little to the resistance change and the CSB in the junction maintains alignment along the wire. When the reversal field is increased to $H_C\sim150$ Oe, a first drop in the resistance occurs in going from B to C, indicating the switching of the CSB close to the diagonal direction. In the field range C to C′, the spin block switches between the two diagonal directions. When the field was further increased to $H_{C'}\sim400$ Oe, the spin block undergoes a second switch between C′and D, leading to a sharp increase of the resistance.

As shown in the straight wires the AMR effect was suppressed in the arms of the 0.5 μm cross and the Lorentz MR is very small. The MR effect observed in the cross comes mainly from two sources: (a) the AMR effect due to the switching of the spin block in the junction, and (b) the possible intrinsic spin-dependent scattering of the electrons propagating through regions of spatially varying magnetization, or the so-called domain-wall MR. The resistance change due to the AMR effect between the configurations B and C can be estimated to be

$$\Delta R/R=(W/D)\mathrm{AMR}_{\mathrm{FeNi}}\cos^2(\theta), \tag{1}$$

where $W=0.5$ μm is the width of the wire and $D=3.4$ μm is the separation of the voltage pads, $\mathrm{AMR}_{\mathrm{FeNi}}=-1.4\%$ is the magnitude of the AMR effect of the 0.5 μm cross determined from transverse MR measurements,[10] and θ is the angle between the spin and the current. As shown in Fig. 4(e) the CSB is expected to be aligned close to the diagonal direction in C, that is $\theta\approx45°$, which gives a MR value of -1.0×10^{-3}. This is much larger than the observed value of $-3.0\pm0.2\times10^{-4}$, indicating a significant contribution of a positive intrinsic MR due to spin dependent scattering of the DW.

To account precisely for the AMR contribution and to exclude any Lorentz MR effect, the magnetization process was further controlled as shown by the MR curve in Fig. 4(c). The field was swept between about -300 to 300 Oe starting from the saturation state A. As the maximum reversal field is smaller than $H_{C'}$, the second jump from C′ to D does not occur in this controlled MR measurement. When the reversal field is reduced to zero, a new configuration B′ strikingly different from that of B was created. The CSB in B′is orientated along the diagonal direction corresponding exactly to the detailed spin configuration established by the results of micromagnetic calculations shown in Fig. 3(a), which allows us to calculate quantitatively the AMR contribution. In addition, any contribution from the Lorentz MR was excluded in zero field.

A numerical calculation of the AMR effect was made by further considering the current distribution in the sample. Figure 3(b) shows the current density distribution calculated using finite element method. The AMR was then calculated as

$$\Delta R/R = \mathrm{AMR}_{\mathrm{FeNi}} \Sigma \cos^2(\theta_i), \tag{2}$$

where θ_i is the angle between the current and magnetization at the unit cell *i*. The resistance change due to the AMR effect between configurations B and B′ is -6.0×10^{-4} integrated over a distance between two voltage pads according to Eq. (2). This value is smaller than that estimated from Eq. (1) which may be due to the fact that about 20% of current flows through the vertical arms and that there is a small perpendicular component of the current within the junction. As the AMR contribution of -6.0×10^{-4} is about twice as large as the measured value of $-3.2\pm0.2\times10^{-4}$, we can thus conclude that the 45° domain wall between the arms and the junction contributes a positive MR with a magnitude of the order of 10^{-4}, i.e., the intrinsic spin-dependent scattering for the electrons propagating through regions of spatially varying magnetization leads to an increase of resistance.

The positive MR effect due to DW scattering is in agreement with the model proposed by Levy and Zhang.[6] In their model, the same Hamiltonian used to explain the GMR effect was used to calculate the resistance change due to the presence of the domain wall. The CSB in the junction behaves like the free layer in a magnetic/nonmagnetic/magnetic/antiferromagnetic spin valve. The domain configuration along either of the wire of the mesoscopic crosses can thus be described as a one-dimensional ''GMR'' structure.

In summary, local magnetotransport measurements are shown to provide a probe of the magnetization process associated with a CSB confined in the submicron junction of mesoscopic NiFe cross-shaped wires. A positive intrinsic MR effect associated with local spin noncollinearity, i.e., the 45° wall between the arms and the junction, in a 0.5 μm cross was unambiguously clarified while the contribution of the AMR effect was excluded by considering the detailed domain configuration and the current distribution. The successful confinement of a CSB using a mesoscopic structure as demonstrated in this work could also open a way to investigate magnetic quantum tunneling[12] in ferromagnetic materials, which are of great current interest.

Recently, two new observations of DW scattering were published. Taniyama *et al.*[13] reported the observation of a negative MR due to the domain wall in Co submicron zigzag wires, in which a 180° DW was assumed to be created. Rüdiger *et al.*[14] made detailed studies on hcp Co films with stripe domains and found that the increase of resistance at the presence of DW (that is positive MR as defined in this paper) found in a previous study[2] is just due to the AMR effect rather than DW scattering, and any intrinsic effect due to DW of this material is very small.

The authors thank Professor A. Fert, Professor P. M. Levy, Dr. W. F. Egelhoff, Jr., Dr. R. McMichael, Dr. U. Rüdiger, and Dr. G. Tatara for helpful discussions. This research was supported by the EPSRC, Newton Trust (Cambridge), Toshiba Corporation, EC program ''MASSDOTS'' (ESPRIT), and ''SUBMAGDEV'' (TMR). C. A. F. Vaz is sponsored by Program PRAXIS XXI (Portugal).

[1] S. S. P. Parkin, Phys. Rev. Lett. **71**, 1641 (1993); T. Lalet and A. Fert, Phys. Rev. B **48**, 7099 (1993).

[2] J. F. Gregg, W. Allen, K. Ounadjela, M. Viret, M. Hehn, S. M. Thompson, and J. M. D. Coey, Phys. Rev. Lett. **77**, 1580 (1996).

[3] K. Hong and N. Giordano, Phys. Rev. B **51**, 9855 (1995).

[4] U. Rüdiger, J. Yu, S. Zhang, A. D. Kent, and S. S. P. Parkin, Phys. Rev. Lett. **80**, 5639 (1998).

[5] Y. Ohtani and K. Fukamichi *et al.*, in *Magnetic Ultrathin Films, Multilayers and Surface—1997*, edited by J. Tobin *et al.*, MRS Symposia Proceedings No. 475 (Materials Research Society, Pittsburgh, 1997), p. 215.

[6] P. M. Levy and S. Zhang, Phys. Rev. Lett. **79**, 5110 (1997).

[7] G. Tatara and H. Fukuyama, Phys. Rev. Lett. **78**, 3773 (1997).

[8] J. B. A. N. van Hoof, K. M. Schep, P. J. Kelley, and G. E. W. Bauer, J. Magn. Magn. Mater. **177**, 188 (1998).

[9] Yuli Lyanda-Geller, I. L. Aleiner, and P. M. Goldbart, Phys. Rev. Lett. **81**, 3215 (1998).

[10] Y. B. Xu and C. A. F. Vaz *et al.*, J. Appl. Phys. **85**, 6178 (1999).

[11] A. O. Adeyeye, G. Lauhoff, J. A. C. Bland, C. Daboo, D. G. Hasko, and H. Ahmed, Appl. Phys. Lett. **70**, 1046 (1997).

[12] Hans-Benjamin Braun, Phys. Rev. B **56**, 8129 (1997); S. Miyashita, K. Saito, and H. De Raedt, Phys. Rev. Lett. **80**, 1525 (1998).

[13] T. Taniyama, I. Nakatani, T. Namikawa, and Y. Yamazaki, Phys. Rev. Lett. **82**, 2780 (1999).

[14] U. Rüdiger, Y. Ju, L. Thomas, S. S. P. Parkin, and A. D. Kent, Phys. Rev. B **59**, 11 914 (1999).